THEORETICAL STUDY OF THE SUBSTITUENT AND SOLVENT EFFECTS ON THE MOLECULAR STRUCTURES, ABSORPTION AND EMISSION SPECTRA OF OPEN-FORM SPIROPYRANS

Yinghong SHENG[1] and Jerzy LESZCZYNSKI[2,*]

The Computational Center for Molecular Structure and Interactions, Department of Chemistry, Jackson State University, P.O. Box 17910, 1400 J. R. Lynch Street, Jackson, MS 39217, U.S.A.; e-mail: [1] yhsheng@ccmsi.us, [2] jerzy@ccmsi.us

Received May 30, 2003
Accepted October 30, 2003

Dedicated to Professor Rudolf Zahradník on the occasion of his 75th birthday.

The effects of substituents and solvents on the molecular structures, excitation energies and emission energies of a series of donor–acceptor substituted spiropyrans were investigated using the density functional methods. Different donor–acceptor pairs lead to alternations of the molecular structures. A relationship between the strengths of donor–acceptor pairs and the structural parameter BLA (bond length alternation) was examined and discussed. The impact on geometrical parameters induced by the solvents is more significant than that caused by the substituents, as indicated by the larger BLA changes. The substituent and solvent effects on the UV absorption and emission spectra of open-form spiropyrans were studied by the TD-DFT method. The absorption maxima of open-form spiropyrans are expected to red shift, and the emission are expected to blue shift as the strengths of donor–acceptor pairs and the polarities of solvents increase. A simple model was adopted to mimic the substituent and solvent effects, in the framework of AM1, employing Sparkles to create an external electric field on the open-form spiropyran, in order to induce a systematical polarization of the molecular equilibrium geometry and the electronic configuration.

Keywords: Spiropyrans; UV-VIS spectroscopy; Emission; Photochromism; Substituent effects; Solvent effects; Time dependent density functional; AM1; BLA; DFT; *Ab initio* calculations.

Spiropyrans are photochromic materials that have been extensively studied due to their potential applications in several important areas, including high-density optical storage, optical switching, image processing, and display[1,2]. The spiropyran comprises a group of light-switchable, photochromic organic molecules. Among various kinds of spiropyrans, 1′,3′,3′-trimethyl-6-nitrospiro[2*H*-1-benzopyran-2,2′-indoline] (6-nitro-BIPS) has been intensively studied[3]. The majority of spiropyrans exist in the dark, in a nonpolar closed form that absorbs light only in the ultraviolet. When exposed to UV

light, the spiropyran undergoes a molecular rearrangement that produces an open form which is colored (absorbing typically at about 530 nm) and highly polar. As shown in Scheme 1, this open form (also called *trans*-merocyanine (MC)) is regarded as a resonance hybrid of a zwitterionic structure and a neutral structure. The open form *trans*-merocyanine can revert back to the closed form thermally or photochemically. Thus, the molecules may be switched from closed to open form (coloration) with UV light (or thermally in the dark in polar solvents) and from open to closed form spiropyran (decoloration) with visible light with typical time scales of microseconds[4].

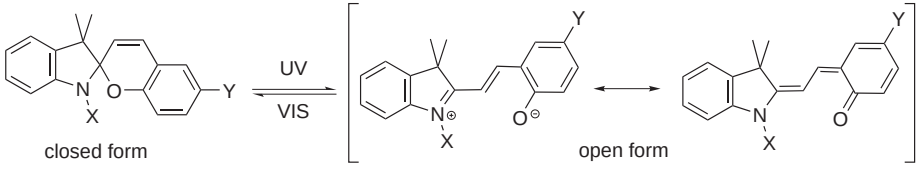

SCHEME 1

The photochromism of the spiropyran/*trans*-merocyanine couple has been reviewed previously[4]. The rate and mechanism of the reaction steps of some spiropyrans and their analogues have been examined with continuous absorption spectroscopy[5], transient absorption spectroscopy, and transient Raman spectroscopy[6]. However, due to its ultrafast feature, the detailed dynamics of spiropyran compounds has not been clarified and a number of unsolved problems remain. For instance, detailed information concerning the geometrical structure as well as the spectrum characteristics of the photochemically produced spiropyrans are still unclear. It is also noticed from the experiments that the substituents and solvents play a very important role in the spectroscopic feature of spiropyrans; however, no systematic theoretical investigation has been carried out so far to study the substituent and solvent effects on the absorption spectroscopy of spiropyrans. Even fewer investigations have been conducted to study the emission spectra of spiropyrans due to the difficulty in treatment of the excited states.

A theoretical investigation of the structure and spectroscopic features of spiropyrans will result in a better understanding of the experimental phenomena and will provide useful information for the rational design of new photochromic compounds with improved performances. Therefore, in this work, we will perform a systematical theoretical study of the spectroscopic properties of a series of open-form spiropyrans with different substituents.

The substitutent and solvent effects on the structures and spectroscopic properties (absorption and emission spectra) are discussed.

METHODOLOGY AND THE MODEL COMPOUNDS

Electronic ground-state geometry optimization. Density functional calculations were carried out to optimize the ground state structures of spiropyran using the B3LYP nonlocal density functional approximation[7]. The 6-31G(d) basis set was applied in most cases since it has been proved to reproduce very well the geometrical parameters. A further expansion of the basis set has less impact[8,9]. We have also used the 6-311+G* basis set and obtained similar geometrical parameters.

It has been reported that for some systems the excitation energies were sensitive to the geometry, so the dependence of geometry on the absorption maxima was also investigated by using the geometries obtained at the HF and MP2 levels. The geometries of spiropyrans in the solvents were re-optimized by the polarized continuum model using the integral equation formalism[10]. Acetone and water were used as solvents.

Excitation energy calculation. The TD-DFT method has been recently shown to yield relatively accurate excitation energies for large molecules[11,12], and in some cases the TD-DFT results are of a quality comparable to that of CAS-PT2 calculations[13] although at substantially lower computational costs. Therefore, the excitation energy calculations were carried out at the TD-DFT level employing the 6-31G(d) basis set, using the B3LYP/6-31G(d) optimized geometries. The 6-311G+(d) and 6-311±G(d,p) basis sets were also used in TDDFT calculations in order to study the basis set effect on the excitation energy. Two different density functionals, B3LYP and BP86, were used in the TD-DFT calculations.

Emission energy calculation. The optimized ground-state geometries can be used for calculation of absorption energies, but the optimization of the first excited state is found to be essential for computation of emission energies[14]. Therefore, the emission energies for selected spiropyrans were calculated by the TD-DFT method using the CIS optimized excited singlet state geometries. All calculations were carried out using the Gaussian 98 program[15].

Model compounds. One of the best known spiropyrans is 1′,3′,3′-trimethyl-6-nitrospiro[2*H*-1-benzopyran-2,2′-indoline] (6-nitro-BIPS). In order to study the substituent effect, several combinations of electron-donating and electron-withdrawing groups (**SP-1**–**SP-4**) were investigated, as shown in Scheme 2. Two donor–acceptor substituted patterns have been investigated. **SP-2** is a weak donor–acceptor substituted spiropyran, while **SP-3** is a stron-

ger donor–acceptor (X = Me, Y = NO_2) substituted spiropyran. For comparison, an unsubstituted (**SP-1**; X = Y = H) and an acceptor–donor substituted spiropyran (**SP-4**; X = MeO, Y = H) were also considered.

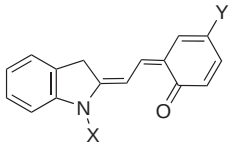

SP-1; X = H, Y = H
SP-2; X = H, Y = NO_2
SP-3; X = Me, Y = NO_2
SP-4; X = H, Y = OMe

SCHEME 2

RESULTS AND DISCUSSION

The Comparison of Excitation Energies at Different Levels of Theory

Using **SP-2** as a model compound, we first studied the dependence of molecular geometries on the excitation energies. The geometries optimized at the B3LYP/6-31G(d), B3LYP/6-31+G(d), HF/6-31G(d), as well as the HF/6-31+G(d) and MP2/6-31G(d) levels were used to calculate the excitation energies. The B3LYP-based TDDFT predicted vertical $n\rightarrow\pi^*$ and $\pi\rightarrow\pi^*$ excitation energies (ΔE), absorption wavelength (λ) and oscillator strengths (f) of spiropyran **SP-2** (X = H, Y = NO_2) at the different molecular geometries are listed in Table I.

The TDDFT predicted absorption maxima (λ_{max}) of its model compound **SP-2** semi-quantitatively reproduce the experimental values which are around 580 nm [2c,6]. All B3LYP based TDDFT predicted absorption maxima amount to about 80% of the experimental value. We also noticed that the B3LYP-based TDDFT predicted λ_{max} at the HF optimized geometry is about 40 nm smaller than that obtained from the B3LYP optimized geometry; therefore, the HF optimized geometry may not be the optimal choice for the excitation energy calculations. The geometry obtained at the MP2 level does not lead to any significant improvement as found in the treatment of the DNA bases elsewhere[16]. Therefore one can conclude that the B3LYP/6-31G(d) optimized geometries can be used to provide reliable excitation energies for the spiropyrans.

The 6-31+G(d) basis set was also used to calculate the excitation energies. As one can see from Table I, the addition of diffuse *s* and *p* functions (6-31+G(d)) only slightly lowers the energy of S_1, while S_2 is slightly raised, by about 0.03 and 0.07 eV, respectively. Larger basis set (6-311+G(d,p)) predicted excitation energies remain essentially unchanged; therefore, the ba-

TABLE I

The predicted vertical n→π* and π→π* excitation energies (Δ*E*, eV), absorption wavelengths (λ, nm) and oscillator strengths (*f*) of open-form spiropyran (**SP-2**; X = H, Y = NO_2) at the different levels of theory

Transition	TDDFT/6-31G(d)[a]			TDDFT/6-31G(d)[b]			TDDFT/6-31+G(d)[b]			TDDFT/6-31G(d)[c]			TDDFT/6-311++G(d,p)[c]		
	Δ*E*	λ	*f*	Δ*E*	λ	*f*	Δ*E*	λ	*f*	Δ*E*	λ	*f*	Δ*E*	λ	*f*
n→π*	2.64	470	0.00	2.48	501	0.00	2.51	494	0.00	2.47	501	0.00	2.52	492	0.00
π→π*	2.77	448	0.74	2.58	481	0.62	2.51	494	0.60	2.59	478	0.62	2.52	492	0.61
π→π*	3.52	353	0.30	3.36	369	0.44	3.30	375	0.48	3.36	369	0.42	3.29	376	0.45
n→π*	3.80	326	0.00	3.54	351	0.00	3.52	352	0.00	3.52	352	0.00	3.49	352	0.00
π→π*	4.03	308	0.12	3.79	327	0.13	3.60	345	0.15	3.73	327	0.13	3.52	345	0.15
n→π*				3.89	319	0.00	3.78	328	0.00	3.83	319	0.00			

[a] Based on HF/6-31G(d) optimized geometry. [b] Based on B3LYP/6-31G(d) optimized geometry. [c] Based on MP2/6-31G(d) optimized geometry.

sis set effect is of less significance. The larger basis sets were also used in other molecular systems, and the results show that the 6-31G(d) basis set qualitatively reproduces the experimental data[17].

The excitation energies predicted by the B3LYP and BP86 density functionals are listed in Table II. It is found that the BP86 functional predicted π→π* excitation energies are closer to the experimental results than the B3LYP-based TDDFT calculated values. The BP86-based TDDFT calculation predicts that the π→π* absorptions are larger than the B3LYP results by about 60 nm and amount to approximately 93% of the experimental value. Therefore we will discuss the excitation energies obtained from the BP86-based TDDFT/6-31G(d) calculation only.

Figure 1 shows the frontier orbitals of the open-form spiropyran **SP-2** at the BP86 level. The lowest transition at 1.66 eV predicted by TD-BP86/6-31G(d) corresponds to the HOMO-1 → LUMO excitation. It is the transition from the lone pair orbital which is located at the O atom of the phenyl group to the LUMO π* orbital; however, such an n→π* transition is largely forbidden due to the planarity of the molecule. Therefore, only the π-type orbitals are shown in Fig. 1. The allowed transition at 2.29 eV (f = 0.37) is a complex π→π* transition with the most contribution coming from the HOMO → LUMO transition. The HOMO-3 → LUMO and HOMO-6 → LUMO transitions contribute about 16% of the total transition energy. The excitation predicted at 2.97 eV which exhibits the strongest os-

TABLE II

The B3LYP and BP86 based TDDFT predicted vertical n→π* and π→π* excitation energies (ΔE, eV), absorption wavelengths (λ, nm) and oscillator strengths (f) of open-form spiropyran (**SP-2**; X = H, Y = NO_2)

TDDFT	B3LYP/6-31G(d)			BP86/6-31G(d)		
	ΔE	λ	f	ΔE	λ	f
n→π*	2.48	501	0.00	1.66	746	0.00
π→π*	2.58	481	0.62	2.29	541	0.37
π→π*	3.36	369	0.44	2.84	437	0.00
n→π*	3.54	351	0.00	2.43	510	0.00
π→π*	3.79	327	0.13	2.97	417	0.54
n→π*	3.89	319	0.00	3.01	412	0.00

* Geometries are optimized at the B3LYP/6-31G(d) level.

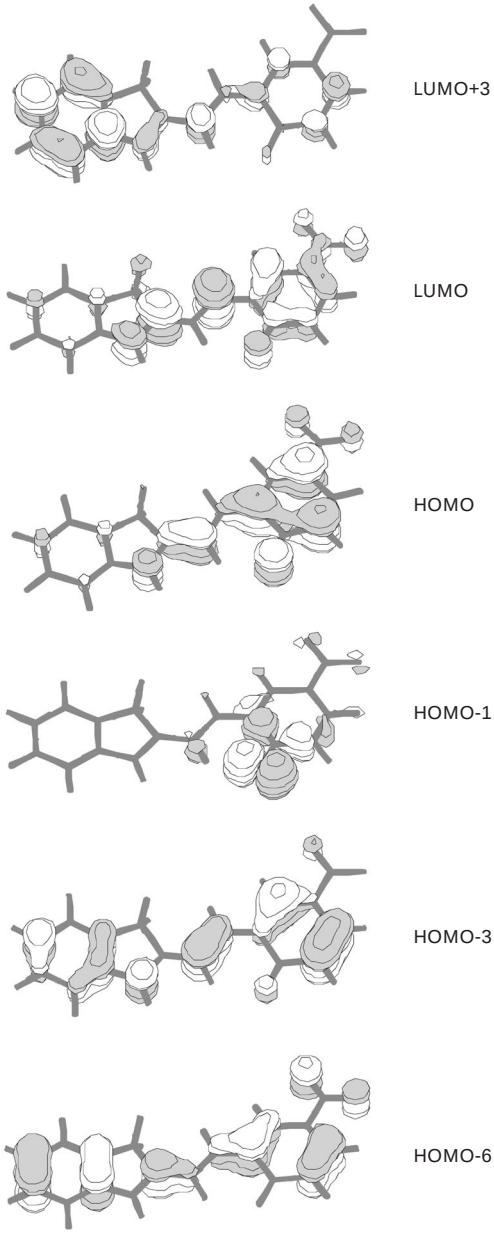

FIG. 1
The selected frontier orbitals of open-form spiropyran **SP-2**

cillator strength (f = 0.54) is also a mixed π→π* transition with 88% of total energy contribution from the HOMO-3 → LUMO transition.

Substituent and Solvent Effects

An introduction of different donor and/or acceptor groups for a π-conjugated open-form spiropyran leads to different changes in the molecular structures. According to the classic valence bond theory[18], the ground state open-form spiropyran can be regarded as a resonance hybrid of a zwitterionic structure and a neutral structure where the degree of mixing of the two structures determines the bond length alternation (BLA) values[19], *i.e.*, the difference between the average lengths of the single and double bonds in the π-conjugated spiropyran. For donor–acceptor spiropyrans, BLA is equal to $(R_{N–C1} + R_{C2–C3} + R_{C4–C5})/3 - (R_{C1–C2} + R_{C3–C4} + R_{C5–C6})/3$. The definition was chosen so that the open-form spiropyrans can be tuned from the neutral resonance form (BLA = +0.1 Å) to the zwitterionic form (BLA = –0.1 Å) with the increasing strength of the donor–acceptor pairs or the polarity of the solvents (Scheme 3). The DFT predicted BLA values for the selected four substituted spiropyrans are listed in Table III. For instance, **SP-4** (X = H, Y = OMe; BLA = 0.043 Å) stands for the neutral spiropyrans, while **SP-3** (X = Me, Y = NO_2; BLA = 0.011 Å) corresponds to the spiropyran with more contribution from the zwitterionic structure.

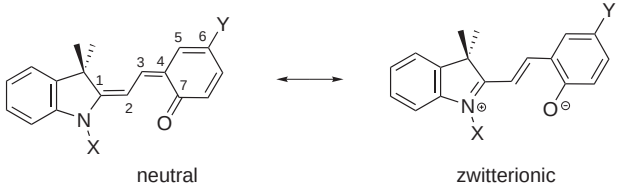

SCHEME 3

The BP86 TDDFT level predicted vertical n→π* and π→π* excitation energies, absorption wavelength and oscillator strengths for spiropyrans **SP-1** to **SP-4** are shown in Table III. The n→π* excitation is largely forbidden; therefore, we will only discuss the π→π* excitation energies. The TD-DFT predicted π→π* excitation energies for **SP-2**, **SP-3** and **SP-4** are around 2.29 eV. Because of its shorter conjugation length, the π→π* excitation energy of **SP-1** (X = Y = H) is relatively smaller. As we described in the preceding section, the π→π* excitation is a mixed π→π* transition with the most energy contributions coming from the HOMO → LUMO transition. It was expected that the π→π* transition would red shift; however, from Table III, one can

TABLE III

The DFT predicted dipole moments (μ, D), BLA values, the BP86 TDDFT predicted vertical n→π* and π→π* excitation energies (Δ*E*, eV), absorption wavelengths (λ, nm) and oscillator strengths (*f*) of the selected four open-form spiropyrans (**SP-1** to **SP-4**). In addition, the BP86 TDDFT predicted absorption spectra of **SP-2** in the acetone and water are also listed

Transition	H-MeO			H-H			H-NO_2			Me-NO_2			H-NO_2(acetone)			H-NO_2(H_2O)		
	Δ*E*	λ	*f*	Δ*E*	λ	*f*	Δ*E*	λ	*f*	Δ*E*	λ	*f*	Δ*E*	λ	*f*	Δ*E*	λ	*f*
n→π*	2.04	609	0.00	1.84	674	0.00	1.66	746	0.00	1.68	740	0.00	1.56	792	0.00	1.50	826	0.00
π→π*	2.29	542	0.42	2.42	512	0.33	2.29	541	0.37	2.28	544	0.39	2.18	568	0.32	2.12	585	0.29
n→π*							2.43	510	0.00	2.44	507	0.00	2.25	552	0.00	2.14	579	0.00
n→π*							2.84	437	0.00	2.84	437	0.00	2.80	443	0.00	2.85	435	0.00
π→π*	3.00	414	0.25	3.03	409	0.23	2.97	417	0.54	2.94	421	0.50	3.01	412	0.64	2.99	415	0.11
n→π*	3.28	378	0.00	3.11	398	0.00	3.01	412	0.00	3.03	410	0.00	3.05	407	0.00			
BLA		0.036			0.033			0.013			0.011			–0.015			–0.030	
μ		5.76			5.66			11.49			11.79			17.04			19.34	

barely see any significant red shift of the $\pi \rightarrow \pi^*$ excitation as observed in the experiments. The reason may be that the donor–acceptor pairs under consideration are not strong enough to lead to significant changes in the structures. A complete evolution of the $\pi \rightarrow \pi^*$ excitation from the neutral to the charge-separated (zwitterionic) limit will be discussed in the following section.

The DFT calculated BLA values and the BP86 TDDFT predicted excitation energies for **SP-2** in acetone and water solvents are also listed in Table III. As one can see from Table III, the BLA value of **SP-2** becomes negative in the acetone and water solvents, and a significant red shift of the $\pi \rightarrow \pi^*$ excitation from the gas phase to the solvents is observed. The λ_{max} value red shifts from 541 nm in the gas phase to 568 and 585 nm in acetone and water, respectively.

Sparkles, Molecular Structures and Excitation Energies

So far, we have studied the variations of transition energies upon adopting different donor–acceptor pairs and in different solvents. The results show that the reference molecular geometry is crucial in determining the molecular optical properties. If one can get systematic changes in molecular structures for a given system, then the variation of optical properties and qualitative effects of donor–acceptor pairs and solvents can be revealed. The key problem is to provide such a complete and systematic polarization of the molecular geometry. To address this problem, a simple approach was proposed, *i.e.*, in the framework of AM1 we adopt Sparkle[20] to produce an external electric field to perturb molecules and produce new equilibrium geometries and electronic configurations[21]. Then the optical properties for this set of equilibrium geometries were investigated.

In this section, we will discuss the study of the properties of **SP-2** under the influence of an external electric field. This electric field was defined by point charges (Sparkles) transferred in steps from each end of the molecule as shown in Scheme 4. The point charges lie perpendicular to the plane of the molecule at the distance (*r*) from the two nitrogen atoms. The Sparkles were set to be $\oplus$ and $\ominus$; the *r* value ranges from 3.0 to 4.1 Å.

At each fixed Sparkle distance (*r*), the molecular geometry was optimized at the AM1 level; the values of the molecular structural parameter (BLA) of the optimized geometries are listed in Table IV.

When Sparkles are moved in steps from 3.0 to 4.1 Å, the molecular structures are tuned from the neutral limit to the zwitterionic limit. The change of dipole moments is consistent with the extent of charge separation which

varies from 9.99 (neutral limit) to 17.20 D (zwitterionic limit) for the real donor–acceptor substituted spiropyrans in the gas phase and solvents as tabulated in Table III.

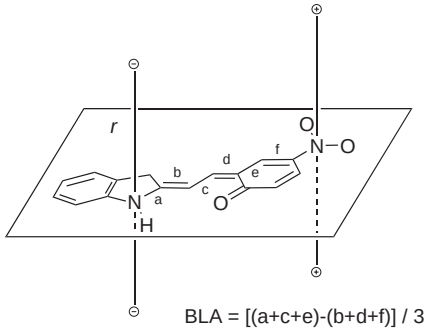

SCHEME 4

Using such obtained sets of equilibrium geometries, the π→π* excitation energy for spiropyran **SP-2** at each fixed Sparkle distance was calculated by the TDDFT method. For comparison, the AM1/CI and ZINDO/S calculated π→π* excitation energies for spiropyran **SP-2** at each fixed Sparkle distance are also shown in Fig. 2 and Table IV. The AM1/CI and ZINDO/S methods yield higher π→π* excitation energies compared to the TDDFT level results.

As one can see from Fig. 2 and Table IV, when the BLA values of **SP-2** decrease from 0.046 Å (the neutral form) to –0.101 Å (the charge-separated form), the TDDFT predicted π→π* excitation energies for spiropyran **SP-2** decrease as is indicated by the red shift of the absorption maxima (λ_{max}) from 557 nm to 635 nm. We also noticed that the λ_{max} values have very slight red shift in the range of BLA = 0.046–0.00 Å. The four selected substi-

TABLE IV
The BP86-TDDFT, AM1/CI and ZINDO/S predicted absorption maxima (λ_{max}, nm) at the AM1 optimized structures at the different *r* values of Sparkles (in Å)

r	BLA	μ_{AM1}	λ_{TDBP86}	λ_{AM1}	$\lambda_{ZINDO/S}$
3.0	0.046	9.99	557	484	478
3.2	0.025	10.98	557	489	478
3.3	0.001	12.18	564	491	480
3.4	–0.035	14.00	582	500	484
4.1	–0.101	17.20	635	506	498

tuted spiropyrans fall in this range which may be the reason why no significant red shift was found in our study.

When BLA changed from 0.00 to –0.101 Å, the λ_{max} values rapidly red shift from 564 to 635 nm. Compared to the values in Table III, one may notice that the BLA value of **SP-2** in an acetone solvent is calculated to be –0.030 Å, while the BLA amounts to –0.035 Å when the *r* distance is 3.4 Å. In both cases, the molecular geometries have similar geometrical parameters, and the λ_{max} values are 585 and 582 nm, respectively. Therefore, the BLA is a key geometrical parameter to determine the optical properties of spiropyrans. This indicates that one can predict the absorption energy of a certain spiropyran by a simple relation to its BLA value.

Emission Energies

The emission energies for **SP-1**, **SP-2**, **SP-3** and **SP-4** are also calculated using the TD-DFT method. Since fluorescence is a relatively slower process, the geometry of the molecule may relax before it decays to the ground state, and the optimization of the first excited state was essential for computations of emission energies[14]. Therefore the fluorescence maxima are calculated using the CIS optimized excited singlet state geometries. The BP86 TDDFT level predicted emission energies, emission wavelength and oscillator strengths are listed in Table V. In experimental studies, the fluorescence maxima of four open-form spiropyran species (SP-methyl, SP-acid, SP-ester, and SP-amide) have been measured in the solvents of different

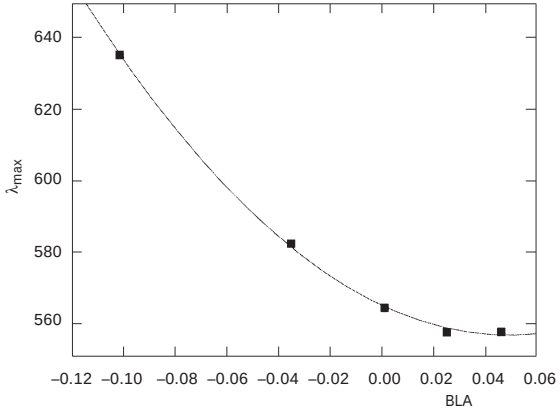

FIG. 2

The relationship between BP86-TDDFT predicted absorption maxima (λ_{max}, nm) *vs* BLA at the AM1 optimized structures at the different *r* values of Sparkles

TABLE V

The BP86- and B3LYP-TDDFT predicted π→π* emission energies (Δ*E*, eV), absorption wavelengths (λ, nm) and oscillator strengths (*f*) of the selected four open-form spiropyrans (**SP-1** to **SP-4**) at the CIS optimized excited singlet state structures

	H-MeO			H-H			H-NO_2			Me-NO_2		
	Δ*E*	λ	*f*	Δ*E*	λ	*f*	Δ*E*	λ	*f*	Δ*E*	λ	*f*
π→π* (BP86-TD)	2.12	585	0.39	2.19	565	0.28	2.17	571	0.34	2.18	568	0.36
π→π* (B3LYP-TD)	2.33	531	0.51	2.42	512	0.42	2.44	508	0.53	2.44	507	0.56
BLA		0.036			0.033			0.013			0.011	

polarities. The emission maxima λ_f of open-form spiropyrans are around 650 nm in nonpolar solvents. It is also observed that the λ_f values of 1′,3′,3′-trimethyl-6-nitrospiro[2*H*-1-benzopyran-2,2′-indoline] blue shifts from 655 to 644 nm as the polarities of solvents increase. The theoretical predicted λ_f in the gas phase is about 87% of the experimental value, indicating that the BP86 method semiquantitatively reproduces the experimental values. Our calculations also reveal the blue shift of the emission bands as the strengths of donor–acceptor pairs increase. For instance, the λ_f value of **SP-1** (X = H, Y = MeO) is 585 nm; it blue shifts to 568 nm for **SP-4** (X = Me, Y = NO_2). Because of the similarities of the solvent and substituent, we expect that the emission in a solvent will also blue shift as the polarities of the solvents increase.

CONCLUSIONS

We have investigated the substituent and solvent effects on the molecular structures, excitation energies and emission energies of a series of donor–acceptor substituted open-form spiropyrans using the density functional methods.

The changes in the molecular structures are found to be related to the geometrical parameter BLA which can be varied from 0.036 to 0.011 Å by adopting different combinations of electron-donating and electron-withdrawing groups. The solvent effect was found to be similar to the substituent effect; however, its impact on the geometrical parameters is much more significant than that of the substituents.

The UV absorptions of selected substituted open-form spiropyrans have been studied by the TDDFT method. The B3LYP based TDDFT predicted $\pi\rightarrow\pi^*$ absorption wavelengths are about 80% of the experimental value, while the BP86-based TDDFT predicted $\pi\rightarrow\pi^*$ absorptions amount to 93% of the experimental value. The absorption maxima of open-form spiropyrans are found to red shift as the strengths of the donor–acceptor pairs and the polarities of the solvents increase; on the contrary, the emission spectra of spiropyrans blue shift.

In addition, a simple model at the AM1 level was adopted to mimic the substituent and solvent effects. This model allows us to study the complete evolution of the molecular spectroscopic features from the neutral limit to the zwitterionic limit, providing helpful information for the rational design of new photochromic compounds with improved performances.

This work was facilitated in part by NSF Grants No. 9805465 & No. 9706268, ONR Grant No. N00014-98-1-0592, EPSCoR Grant No. 55-98-1-0247, NSF Grant CTS-0102680, and the Army High Performance Computing Research Center under the auspices of the Department of the Army, Army Research Laboratory cooperative agreement No. DAAH04-95-2-0003/contract No. DAAH04-95-C-0008. This work does not necessarily reflect the policy of the government, and no official endorsement should be inferred. We would like to thank the Mississippi Center for Supercomputing Research for a generous allotment of computer time.

REFERENCES

1. Willner I., Katz E., Willner B., Blonder R., Heleg-Shabtai V., Buckman A. F.: *Biosens. Bioelectron.* **1997**, *12*, 337.
2. a) Willner I.: *Acc. Chem. Res.* **1997**, *30*, 347; b) Willner I., Rubin S., Shatzmiller R., Zor T.: *J. Am. Chem. Soc.* **1993**, *115*, 8690; c) Garcia A. A., Cherian S., Park J., Gust D., Jahnke F., Rosario R.: *J. Phys. Chem.* **2000**, *104*, 103.
3. a) Guglielmetti R. in: *Photochromism – Molecules and Systems, Studies in Organic Chemistry* (H. Durr and H. Bouas-Laurent, Eds), Vol. 40, pp. 314, 493, 879. Elsevier, Amsterdam 1990; b) Crano J. C., Guglielmetti R. (Eds): *Organic Photochromic and Thermocheromic Compounds*, Vols 1 and 2. Plenum Press, New York 1999.
4. Becker R. S., Michl J.: *J. Am. Chem. Soc.* **1996**, *88*, 5931.
5. a) Salemi-Delvaux C., Luccioni-Houze B., Baillet G., Giusti G., Gugllemetti R.: *J. Photochem. Photobiol. A: Chem.* **1995**, *91*, 223; b) Pimienta V., Lavabre D., Levy G., Samat A., Guglielmetti R., Micheau J. C.: *J. Phys. Chem.* **1996**, *100*, 4485; c) Tamai N., Miyasaka H.: *Chem. Rev.* **2000**, *100*, 1875.
6. a) Chibisov A. K., Görner H.: *J. Phys. Chem. A* **1997**, *101*, 4305; b) Görner H.: *Phys. Chem. Chem. Phys.* **2001**, *3*, 416.
7. a) Lee C., Yang W., Parr R.: *Phys. Rev. B: Condens. Matter* **1988**, *37*, 785; b) Becke A. D.: *J. Chem. Phys.* **1993**, *98*, 5648; c) Miehlich B., Savin A., Stoll H., Preuss H.: *Chem. Phys. Lett.* **1989**, *90*, 5622.
8. a) Hariharan P. C., Pople J. A.: *Chem. Phys. Lett.* **1972**, *66*, 217; b) Hehre W. J., Radom L., Schleyer P. v. R., Pople J. A.: *Ab initio Molecular Orbital Theory*. Wiley, New York 1986.
9. a) Holmén A., Broo A.: *Int. J. Quantum Chem.* **1995**, *QBS22*, 113; b) Broo A., Holmén A.: *Chem. Phys.* **1996**, *211*, 147; c) Broo A.: *Int. J. Quantum Chem.* **2000**, *77*, 454.
10. Cances M. T., Mennucci V., Tomasi J.: *J. Chem. Phys.* **1997**, *107*, 3032.
11. a) Bauernschmitt R., Ahlrichs R.: *Chem. Phys. Lett.* **1996**, *256*, 454; b) Straman R. E., Scuseria G. E., Frisch M. J.: *J. Chem. Phys.* **1998**, *109*, 8218.
12. Han Y.-K., Lee S. U.: *Chem. Phys. Lett.* **2002**, *366*, 9.
13. Serrano-Andres L., Merchan M., Rubio M., Roos B. O.: *Chem. Phys. Lett.* **1998**, *295*, 195.
14. Parusel A. B., Rettig W., Sudholt W.: *J. Phys. Chem.* **2002**, *106*, 804.
15. Frisch M. J., Trucks G. W., Schlegel H. B., Scuseria G. E., Robb M. A., Cheeseman J. R., Zakrzewski V. G., Montgomery J. A., Jr., Stratmann R. E., Burant J. C., Dapprich S., Millam J. M., Daniels A. D., Kudin K. N., Strain M. C., Farkas O., Tomasi J., Barone V., Cossi M., Cammi R., Mennucci B., Pomelli C., Adamo C., Clifford S., Ochterski J., Petersson G. A., Ayala P. Y., Cui Q., Morokuma K., Malick D. K., Rabuck A. D., Raghavachari K., Foresman J. B., Cioslowski J., Ortiz J. V., Baboul A. G., Stefanov B. B., Liu G., Liashenko A., Piskorz P., Komaromi I., Gomperts R., Martin R. L., Fox D. J., Keith T., Al-Laham M. A., Peng C. Y., Nanayakkara A., Gonzalez C., Challacombe M.,

Gill P. M. W., Johnson B. G., Chen W., Wong M. W., Andres J. L., Head-Gordon M., Replogle E. S., Pople J. A.: *Gaussian 98*, Revision A.10. Gaussian Inc., Pittsburgh (PA) 1998.
16. Broo A., Holmén A.: *J. Phys. Chem. A* **1997**, *101*, 3589.
17. a) Neiss C., Saalfrank P., Parac M., Grimme S.: *J. Phys. Chem. A* **2003**, *107*, 140; b) Parac M., Grimme S.: *J. Phys. Chem. A* **2002**, *106*, 6844; c) Furche F., Ahlrichs R., Wachsmann C., Weber E., Sobanski A., Vögtle F., Grimme S.: *J. Am. Chem. Soc.* **2002**, *122*, 1717; d) Parusel A. B. J., Rettig W., Sudholt W.: *J. Phys. Chem. A* **2002**, *106*, 804.
18. Brooker L. G. S., Keyes G. H., Sprague R. H., Vandyke R. H., Vanlare E., Vanzandt G., White F. L., Cressman H. W. J., Dent S. G.: *J. Am. Chem. Soc.* **1951**, *73*, 5332.
19. a) Meyers F., Marder S. R., Pierce B. M., Brédas J. L.: *J. Am. Chem. Soc.* **1994**, *116*, 10703; b) Marder S. R., Gorman C. B., Meyers F., Perry J. W., Bourhill G., Brédas J. L., Pierce B. M.: *Science* **1994**, *265*, 632; c) Sheng Y., Jiang Y., Wang X.-C.: *J. Chem. Soc., Faraday Trans.* **1998**, *94*, 47.
20. Stewart J. J. P., Frank J.: Seiler Research Laboratory, U.S. Air Force Academy, Colorado Springs, CO 80840, U.S.A.
21. a) Gorman C. B., Marder S. R.: *Proc. Natl. Acad. Sci. U.S.A.* **1993**, *90*, 11297; b) Sheng Y., Jiang Y.: *J. Chem. Soc., Faraday Trans.* **1998**, *94*, 1929.